LUT University

Effect of thiourea on electrocrystallization of Cu–Sn alloys from sulphate electrolytes

Kasach Aliaksandr A., Kharitonov Dmitry S., Makarova Irina V., Wrzesińska Angelika, Zharskii Ivan M., Kurilo Irina I.

This is a Post-print version of a publication

published by Elsevier

in Surface and Coatings Technology

DOI: 10.1016/j.surfcoat.2020.126137

Copyright of the original publication: © 2020 Elsevier

Please cite the publication as follows:

Kasach, A. A., Kharitonov, D. S., Makarova, I. V., Wrzesińska, A., Zharskii, I. M., Kurilo, I. I. (2020). Effect of thiourea on electrocrystallization of Cu–Sn alloys from sulphate electrolytes. Surface and Coatings Technology, vol. 399. DOI: 10.1016/j.surfcoat.2020.126137

This is a parallel published version of an original publication. This version can differ from the original published article.

Effect of Thiourea on Electrocrystallization of Cu–Sn Alloys from Sulphate Electrolytes

Aliaksandr A. Kasach[a,*], Dmitry S. Kharitonov[a,b,*], Irina V. Makarova[c], Angelika Wrzesińska[d], Ivan M. Zharskii[a], and Irina I. Kurilo[e]

[a]Department of Chemistry, Electrochemical Production Technology and Materials for Electronic Equipment, Belarusian State Technological University, Sverdlova 13a, 220006 Minsk, Belarus

[b]Soft Matter Nanostructures Group, Jerzy Haber Institute of Catalysis and Surface Chemistry, Polish Academy of Sciences, Niezapominajek 8, PL 30-239 Krakow, Poland

[c]Department of Separation and Purification, Lappeenranta University of Technology, Yliopistonkatu 34, FI 53-850 Lappeenranta, Finland

[d]Department of Molecular Physics, Lodz University of Technology, Żeromskiego 116, PL 90-924 Lodz, Poland.

[a]Department of Physical, Colloid and Analytical Chemistry, Belarusian State Technological University, Sverdlova 13a, 220006 Minsk, Belarus

[*]Corresponding authors:

Aliaksandr A. Kasach: kasach2018@bk.ru; ORCID: 0000-0001-5522-2928

Dmitry S. Kharitonov: nckharyt@cyf-kr.edu.pl; ORCID: 0000-0003-2071-3975; Tel +48782037574

Abstract

In this work, the effect of thiourea on the initial stages of the Cu–Sn electrodeposition in the potential range of the underpotential deposition (UPD) of tin from the sulphate electrolyte was studied by linear sweep voltammetry. The mechanism of Cu–Sn alloy nucleation and growth was proposed based on the results of chronoamperometry, chronopotentiometry, and scanning electron microscopy. Thiourea in the concentrations of 0.001–0.010 g/L showed a significant inhibitory effect on the reduction of copper ions. Analysis of the current-time dependencies revealed that Cu–Sn deposition in the UPD region of tin from thiourea-containing solutions proceeds through 3D diffusion-controlled growth of copper clusters. The nucleation type and the main nucleation parameters were calculated based on the Scharifker and Hills theoretical model. Galvanostatic experiments proved that the UPD of tin occurs on the surface of initially formed copper clusters. Surface characterization of Cu–Sn coatings deposited in the presence of thiourea showed a good correlation with electrochemical experiments.

Keywords: nucleation; copper-tin alloy; underpotential deposition; electrocrystallization mechanism

1. Introduction

Copper-tin alloys (5–20 wt% Sn) are widely used in industry as structural elements, machine tools, bearings, fasteners, and electrical contacts owing to their outstanding corrosion resistance, ductility, microhardness, and electroconductivity [1–3]. The growing interest in this type of coating is essentially connected with the strict regulations of the nickel use in European countries. Nickel salts are included in the list of carcinogenic, mutagenic, or toxic to reproduction (CRM) substances (EC Regulation No 790/2009), while products of Ni corrosion can cause allergic reactions in contact with human skin [3–8].

Electrodeposition is a convenient and low-cost technique usually used to obtain copper-based alloys with controllable surface and engineering properties. Acidic or alkaline baths could be used for the deposition of commercial Cu–Sn coatings [9]. For several decades, highly toxic cyanide-based electrolytes were widely used for electrodeposition of copper-tin alloys [2,10]. Recently, sulphate [3,11–15], pyrophosphate [16,17], methanesulfonic [9,18–21], oxalic acid [22,23], and non-aqueous [1,24] electrolytes have been proposed. The use of mentioned compositions can significantly reduce the negative environmental impact. Overall, the most affordable, cheap, and easy-to-operate electrolytes used today are acidic electrolytes for electrodeposition of yellow bronzes. Proposed compositions are based on salts of copper and tin and necessarily include special organic additives. Yellow bronzes containing up to 20 wt% of Sn have been obtained in sulphate electrolytes containing gelatin,[3] gluconic acid [11], polyethylene glycol [12], and benzaldehyde [13]. Thiourea (TU) is one of the most effective organic additives introduced into sulphate electrolytes of Cu and Cu–Sn plating because it increases cathodic polarization by chelating copper ions, imparts an appealing appearance, and assists in the deposition of fine crystalline coatings [20,22–24].

Despite certain progress in the understanding of the kinetics of independent electrodeposition of copper and tin, the process of Cu–Sn bronze formation has been studied not so wide. The presence of

organic additives has a substantial inhibitory effect on the reduction kinetics of aquated copper and stannous ions. Furthermore, Survila et al. reported that the deposition of tin from such electrolytes proceeds on the underpotential deposition (UPD) mechanism (i.e. deposition occurs at potentials more positive than the equilibrium potential for the reduction reaction) [11–13]. In the case of UPD of metals, the formation of two-dimensional structures with a thickness of several atoms has been reported [25,26]. However, UPD of tin was observed in a potential range where copper ions are discharged at the diffusion-limited current (DLC) [15,27]. Therefore, the growth of copper clusters is the determining factor affecting the microstructure of the deposited alloy.

To the best of our knowledge, no studies on the effect of TU on the mechanisms of electrochemical nucleation of Cu–Sn alloys from sulphate electrolytes have been reported in the literature. Understanding of mechanisms and main kinetic parameters of electrocrystallization of alloys opens wide possibilities to obtain multilayered structures, with both improved corrosion [28,29] and physicomechanical properties [30].

In this paper, we showed the effect of TU on the nucleation and clarified the mechanism of copper-tin alloy electrodeposition from the sulphate electrolyte in the region of the UPD of tin under potentiostatic and galvanostatic conditions using several analytical methods, such as scanning electron microscopy (SEM), atomic force microscopy (AFM), energy-dispersive X-ray spectroscopy (EDX), and X-ray diffraction (XRD).

2. Experimental

Electrochemical experiments were performed using an AUTOLAB PGSTAT302N galvanostat-potentiostat in a standard three-electrode glass electrochemical cell. The electrochemical deposition of Cu–Sn alloys was performed from the electrolyte of the following composition: 40 g/L $CuSO_4 \cdot 5H_2O$, 40 g/L $SnSO_4$, and 100 g/L H_2SO_4. The concentration of TU in the electrolyte was varied in the range of 0.001–0.010 g/L. The chemicals of analytically pure grade (Belreachim, Belarus) were used as received. To study the effect of TU on the kinetics of cathodic reduction of an individual alloy component, electrolytes of a similar composition containing the salt of only one of the deposited metals (copper or tin) were prepared. A new portion of the electrolyte was used in each experiment. Copper plates with relative surface ratio 1/9 (cm^2) were used as cathodes and anodes. The distance between electrodes was 3 cm. The parameters of electrolysis (current density or potential, and duration) used in the experiments are reported in the text. The temperature during all electrochemical experiments was maintained at 20°C using a VT3−1 thermostat. Prior to each experiment, the cathode surface was ground with P4000 emery paper and chemically prepared according to ISO 27831-2:2008: degreased in the solution containing 15 g/L Na_2CO_3, 30 g/L $Na_3PO_4 \cdot 12H_2O$, and 5 g/L Sintanol DS10 and then activated in 0.1 M H_2SO_4. Before experiments, electrolytes were stirred for 5 min and then stirring was switched off.

Linear sweep voltammetry (LSV) was used to determine the kinetics of electrochemical processes occurring in electrolytes under study. In these experiments, a saturated silver/silver chloride electrode was used as the reference electrode and a copper foil (99.9%, 9 cm^2) was used as the counter electrode. All measured potentials are reported on the scale of the standard hydrogen electrode (SHE). Experiments were performed in the potential range of 300–(–230) mV (Cu and Cu–Sn deposition) and –190–(–230) mV (Sn deposition) at a linear potential sweep rate of 1 mV/s. All electrochemical experiments reported in this study were at least triplicated.

The morphology and composition of the formed coatings were examined using a JSM-5610 LV scanning electron microscope equipped with an EDX JED-2201 JEOL chemical analysis system. XRD analysis of the phase composition of the deposited coatings was carried out using a D8 Advance AXS X-ray diffractometer with Cu$K\alpha$ radiation (λ= 0.15418 nm) at 40 kV and 30 mA. Processing of the obtained diffraction patterns was carried out using the *Match!* Software and the COD (Crystallography Open Database) reference base. The average crystallite size was calculated using the Scherrer equation (software EVA, version 5.1), as follows:

$$d=0.9\cdot\lambda/b\cdot\cos\Theta$$

where b is the FWHM, θ is the diffraction angle, d is the grain size, and λ (0.15405 nm) is the wavelength of the radiation used.

AFM topography images were obtained in the tapping mode using a Nanosurf Flex-Axiom atomic force microscopy system. An *n*-type silicon cantilever with a nominal tip radius of 8 nm (HQ:NSC15/Al, MikroMasch) was used. The measured areas contained 256×256 data points and were analyzed using the *Gwyddion 2.50* software. The surface roughness was expressed by an average deviation parameter (R_a) on the 10 μm length as an average of 5 measurements.

3. Results and Discussion

3.1 Reduction of Cu(II), Sn(II), and Cu(II)+Sn(II) ions in thiourea-containing sulphate electrolyte

Figure 1 shows cathodic LSV curves of the copper electrode, characterizing the effect of TU on the kinetics of cathodic deposition of copper (Fig. 1a), tin (Fig. 1b), and copper-tin alloy (Fig. 1c). In the

sulphate electrolyte without TU (Fig. 1a), reduction of copper ions occurs in the potential range of 300–80 mV that is typical for this type of electrolyte [31–33]. The addition of TU in the electrolyte (Fig. 1a) results in a shift of polarization curves by 30–210 mV towards more negative potentials at a cathodic current density of –0.005 A/cm^2. The observed decreases in the potential in the presence of TU suggest inhibition of the electroreduction of copper ions. At potentials lower than 40 mV, a diffusion-limited plateau corresponding to the cathodic current density of –0.012 A/cm^2 was observed on LSV curves.

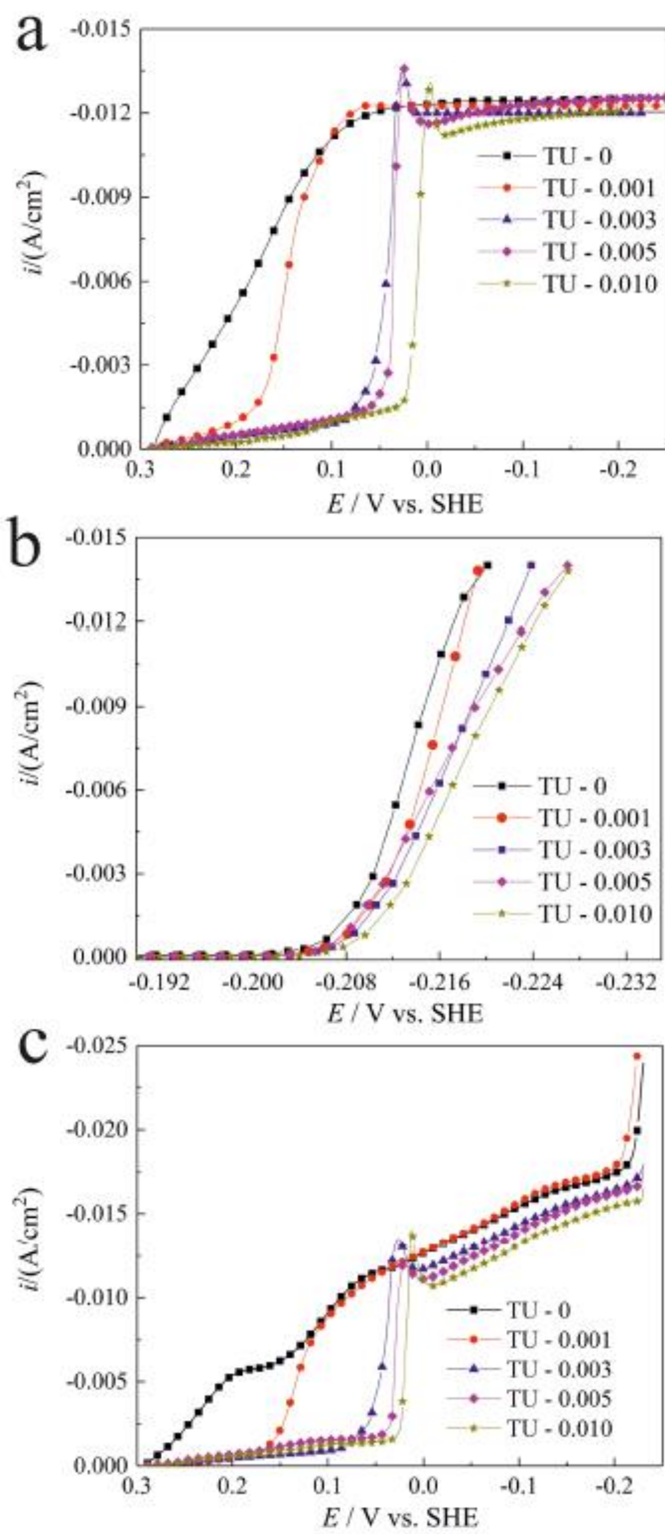

Fig. 1. Linear sweep voltammetry curves characterizing reduction of (a) Cu^{2+}, (b) Sn^{2+}, and (c) simultaneously Cu^{2+} and Sn^{2+} ions in the sulphate electrolyte with and without TU.

Polarization curves of cathodic deposition of tin (Fig. 1b) show that the reduction of stannous ions initiates at potentials lower than –200 mV. The addition of small amounts of TU (Fig. 1b) leads to the shift of the polarization dependences by 10–20 mV towards negative potentials. This value is much lower than that observed for the reduction of copper ions and indicates only a slight inhibition of the reduction process of stannous ions.

In the case of electrolyte, containing both copper and stannous ions (Fig. 1c), a change in the slope of the DLC regions where copper ions are reduced at the limiting current, can be seen on polarization dependences. This regularity can be attributed to the UPD of tin [15]. It is well known that the electrochemical deposition of several metals (or alloys) at a cathode from simple electrolytes is possible only if the difference between the standard reduction potentials of these metals is small (26.5 mV in the case of two-electron transfer processes) [34]. Nevertheless, deposition of the Cu–Sn alloy from the sulphate electrolyte occurs at more noble potentials relative to the standard reduction potential of the $Sn^{2+}|Sn^0$ system (–140 mV), suggesting the UPD of tin. Summarizing, polarization results revealed that in the examined concentrations TU inhibits only the reduction of copper ions. As the deposition of copper and tin was performed on the same substrate in the same experimental conditions, this difference is most probably due to the formation of stable Cu–TU complexes during electrolysis, which can be adsorbed on the surface, inhibiting the reduction process of copper ions [35,36]. Effective inhibition of the reduction of stannous ions by TU has been reported in the literature starting from 1 g/L of TU in the deposition bath [37,38].

3.2 Mechanism of Cu–Sn electrocrystallization

To study the effect of TU on the initial stages of the electrocrystallization of the Cu–Sn alloy in the region of the UPD of tin, chronoamperograms at the fixed potential of –50 mV in the sulphate electrolyte were obtained (Fig. 2). At the initial stage, the recorded *i*–*t* curves in the TU-free electrolyte shows long-time decreasing of cathodic current that cannot be attributed to double-layer charging because it extends over 10 s. In this case, no sign of current maxima at the *i*–*t* dependence may indicate that primary planar subcritical nanoclusters are being formed, which are not contributing to an increase in active surface area [39,40].

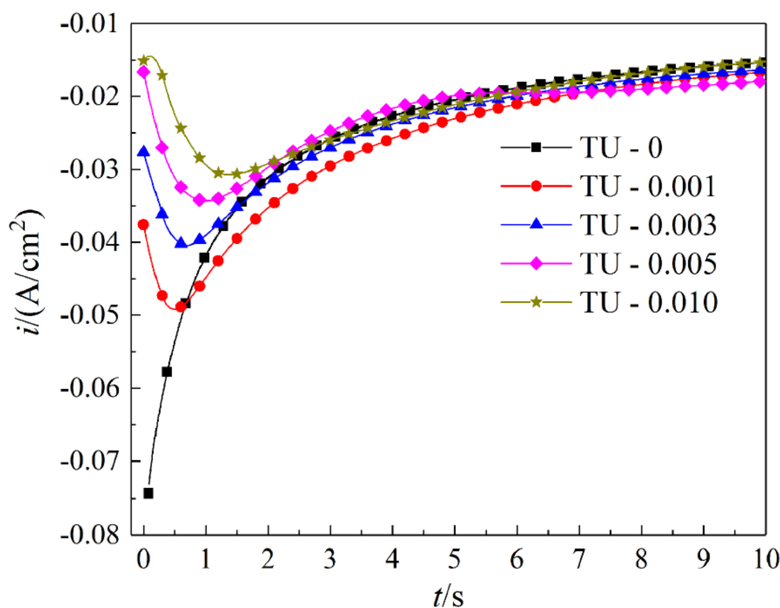

Fig. 2. Chronoamperograms of copper electrode in sulphate electrolyte of Cu–Sn deposition with and without TU.

The TU introduction into the electrolyte changed the appearance of the chronoamperograms. The *i*–*t* curves are characterized by an initial current increase with a pronounced peak characteristic for

nucleation [41]. The maximum current is followed by a decreasing part with the final convergence of the curves to the limiting current, which is typical for a diffusional control. The nucleation and growth of Cu–Sn clusters, in this case, is following the three-dimensional (3D) mechanism [39,40,42,43]. According to this model, an increase in the cathodic current density is the result of the increased true surface area of the electrode. A further decrease in the current density with time is due to the overlapping of the diffusion zones of growing clusters. As a result, the true electrode surface area strives to its geometric value [39,44,45].

To clarify the mechanism of Cu–Sn alloy deposition in the presence of TU, chronoamperograms obtained in the sulphate solutions containing either copper and stannous ions or only copper ions are presented in Fig. 3. In the initial moment (up to 1.5 s for electrolytes without TU and 3.0 s for electrolytes containing 0.001 g/L of TU), recorded chronoamperograms in both solutions overlap each other. This is an important point indicating that the formation of only copper clusters occurs in both electrolytes in the first several seconds of potentiostatic electrolysis. Afterward, the total current density in the solution containing copper and stannous ions increases due to the contribution of the UPD of tin. After 30 s of electrolysis, the cathodic current density of 0.012 A/cm^2, corresponding to DLC of copper ions reduction, was recorded in the individual copper plating electrolyte (inset in Fig. 3). In the case of the electrolyte containing both copper and stannous ions, a DLC plateau was observed at the cathodic current density of 0.014 A/cm^2. Summarizing, one can conclude that in the sulphate electrolyte containing Cu^{2+}, Sn^{2+}, and TU, nucleation proceeds on the 3D mechanism and is followed with the diffusion-controlled growth of copper clusters. Then the UPD of tin occurs on the surface of the formed copper clusters.

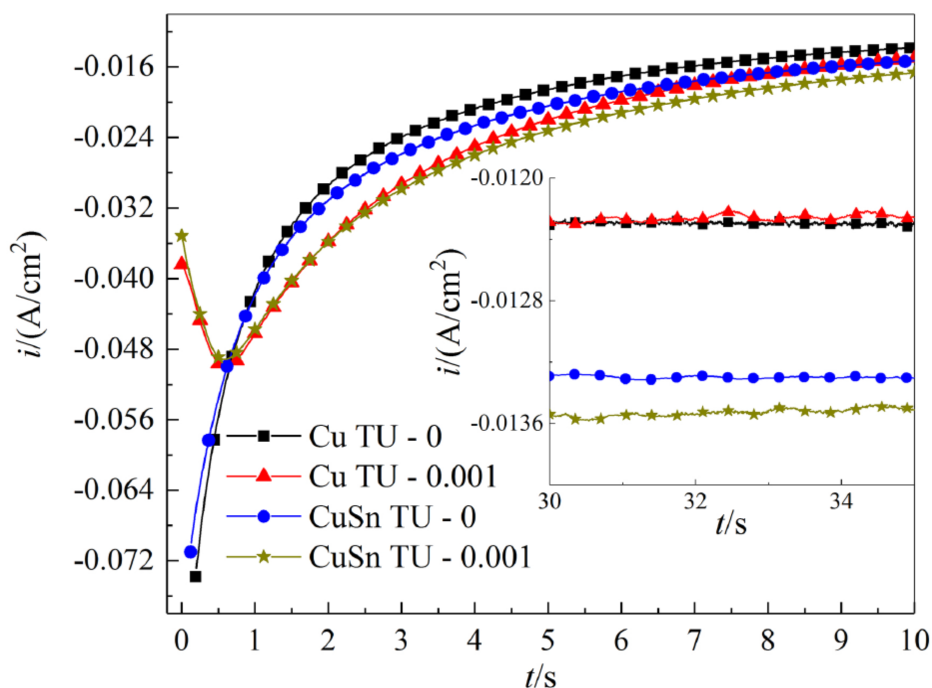

Fig. 3. Chronoamperograms of copper electrode in the sulphate electrolyte containing Cu^{2+}, and simultaneously Cu^{2+} and Sn^{2+} ions with and without TU. Inset shows enlarged view after 30 s of experiment.

Obtained chronoamperograms can be used to determine the nucleation mechanism and parameters related to nucleation [46,47]. To determine the type of copper nucleation in sulphate electrolyte of Cu–Sn deposition containing 0.001–0.010 g/L of TU, the corresponding chronoamperograms (Fig. 2) were presented in the coordinates i^2/i_m^2 (i_m is the maximum current) vs t/t_m (t_m is the moment when the maximum current was recorded). Chronoamperograms in the solutions without TU did not show a current maximum and thus were not examined. The obtained current transients are shown in Fig. 4. The analysis of the transients was performed using the model developed by Scharifker and Hills [46,48,49]. The experimental data were compared with theoretical dimensionless curves for the diffusion-controlled

instantaneous (Eq. 1) and progressive (Eq. 2) nucleation, which were plotted using the equations below [47,48,50]:

$$\frac{i^2}{i_m^2}=1.9542\left(\frac{t_m}{t}\right)\left[1-\exp\left(-1.2564\frac{t}{t_m}\right)\right]^2 \quad (1)$$

$$\frac{i^2}{i_m^2}=1.2254\left(\frac{t_m}{t}\right)\left[1-\exp\left(-2.3367\frac{t^2}{t_m^2}\right)\right]^2 \quad (2)$$

In the case when potentials of Cu–Sn alloy deposition are in the region of the UPD of Sn, the formation of copper crystallization centers from electrolytes containing 0.001 to 0.005 g/L of TU is described by the instantaneous nucleation model, which corresponds to growth of a constant number of supercritical clusters on a small number of active sites formed at the beginning of the electric pulse [47]. The current transient obtained for higher TU concentration (0.010 g/L) did not follow the instantaneous nucleation model. In this case, experimental data initially is well described by the progressive nucleation model, where new nuclei appear during the whole period of deposition but lay between the two theoretical cases afterward. A change to the progressive nucleation can be associated either with the solution chemistry, i.e. formation of more stable Cu–TU complex species, or a modification of the substrate by an inhibiting layer of adsorbed TU, which decelerates the growth of nuclei [36,38]. The deviation from the theoretical transient may be explained by the mixed kinetic/diffusion control of the electrodeposition process [44].

Based on the theoretical nucleation models it is also possible to calculate the diffusion coefficient D of copper(II) ions, the nuclei density N_0 (for the instantaneous nucleation), and nucleation rate J_{nucl} (for the progressive nucleation) of copper in the studied solutions. In the case of instantaneous nucleation, the diffusion coefficient D and the nuclei density N_0 can be given as follows [46,49]:

$$D = \frac{i_m^2 t_m}{0.1629(zFc)^2} \tag{3}$$

$$N_0 = 0.065\left(\frac{1}{8\pi c V_m}\right)^{1/2}\left(\frac{zFc}{i_m t_m}\right)^2 \tag{4}$$

For the progressive nucleation, D and J_{nucl} were determined as [46]:

$$D = \frac{i_m^2 t_m}{0.2898(zFc)^2} \tag{5}$$

$$J_{\text{nucl}} = AN_0 = 0.2898\frac{(zFc)^2}{(8\pi c V_m)^{1/2}\, i_m^2 t_m^3} \tag{6}$$

In these equations, A is the nucleation rate constant, N_0 is the number density of active sites, zF is the molar charge transferred during electrodeposition, c is the concentration of copper ions in the bulk solution, and V_m is the molar volume of the deposited metal. The calculated parameters for current transients in the presence of TU are listed in Table 1. The results show that with increasing concentration of TU the nucleation rate of copper decreased. These observations are in good agreement with data reported in the literature on the deposition of bulk copper on Au (111) [42], *n*-Si (111) [43], and stainless steel [51] in the presence of TU. The apparent slight decrease of the diffusion coefficient in the solution containing 0.010 g/L of TU may be explained by the application of the progressive nucleation model.

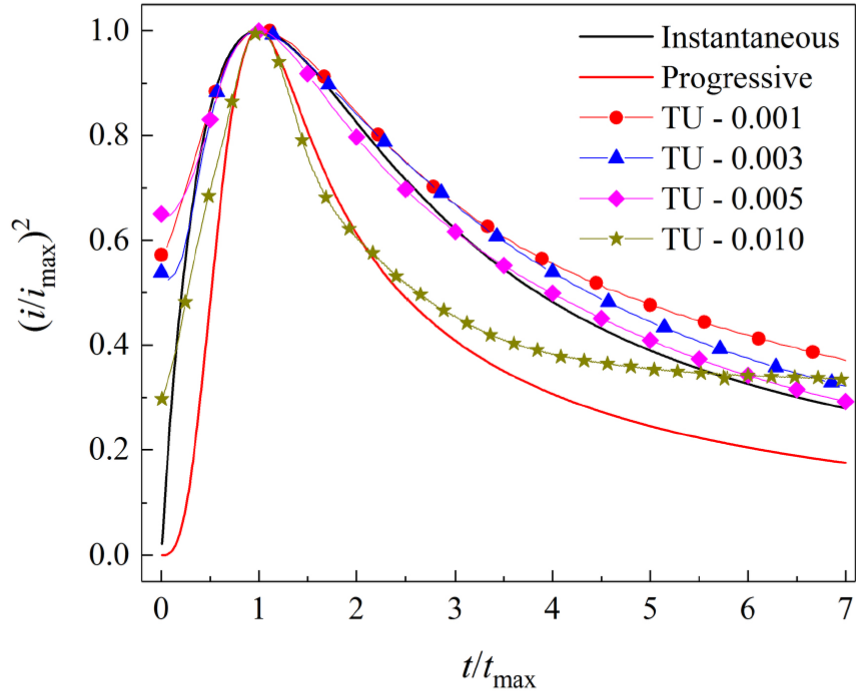

Fig. 4. Dimensionless transients for copper reduction in the sulphate electrolyte containing simultaneously Cu^{2+} and Sn^{2+} ions. Theoretical transients of instantaneous and progressive nucleation were calculated from Eqs (1, 2).

Table 1. Parameters of current transients calculated from Eqs. (3–6)

C_{TU}, g/L	t_m, s	i_m, A/cm^2	D, cm^2/s	N_0, 1/cm^2	J_{nucl}, 1/(cm^2·s)
0.001	0.49 ± 0.04	–0.045 ± 0.003	(2.62 ± 0.60) × 10^{-6}	(1.52 ± 0.42) × 10^6	–
0.003	0.84 ± 0.09	–0.042 ± 0.005	(3.91 ± 1.51) × 10^{-6}	(0.61 ± 0.24) × 10^6	–
0.005	1.04 ± 0.19	–0.035 ± 0.006	(3.36 ± 2.09) × 10^{-6}	(0.59 ± 0.31) × 10^6	–
0.010	1.51 ± 0.32	–0.031 ± 0.004	(2.40 ± 1.31) × 10^{-6}	–	(1.33 ± 0.90) × 10^6

To evaluate the theoretical predictions, Cu–Sn coatings were electrodeposited at the potential of −50 mV for 0.8 s in the same experimental conditions (cell geometry, surface preparation, etc.) and examined by SEM (Fig. 5). For comparison, SEM image of as-polished substrate is also provided (Fig. 5a). Planar structures were formed from the electrolyte without TU (Fig. 5b, b*), which is consistent with the results of chronoamperometry (Fig. 2), where no pronounced current maxima was recorded at the *i*–*t* dependence, indicating formation of planar nanoclusters. Introduction of TU into the electrolyte results in a significant difference in morphology. When 0.001 g/L of TU was added to the electrolyte (Fig. 5c), the formation of clusters with ca. 100 nm in diameter was observed. Side-view SEM image (Fig. 5c*) supports the 3D nucleation mechanism. A further increase in the TU content (Fig. 5d–f) resulted in a decrease in the size of the formed clusters up to 20 nm while increasing their number. Moreover, the actual nuclei densities estimated from SEM images were greater by several orders of magnitude than those predicted by the model (Table 1). The reason of such inconsistency between theoretical calculations and experimental observations can be the effect of TU on electrocrystallization: (1) the organic additive is adsorbed on the surface of growing clusters suppressing their growth and (2) simultaneously favoring the formation of new nuclei. The process of the adsorption of ions onto the electrode surface, followed by surface diffusion and nucleation, which can occur parallel to conventional growth by attachment of ions from the electrolyte onto existing clusters, must be also considered. Adsorption is expected to be important only at early stages, since direct supply of ions to the surface will be reduced once the diffusion fields around the clusters overlap [52]. Moreover, the number of growing clusters, i.e., those that can be experimentally observed by SEM, do not reflect only nucleation, but also aggregation kinetics [40]. Although observing the individual nuclei in a cluster of overlapping nuclei on SEM images is somehow challenging, this method is more accurate than the mathematical equations. Deviation of the nuclei population density and size from those predicted by the models has been reported in the literature [41].

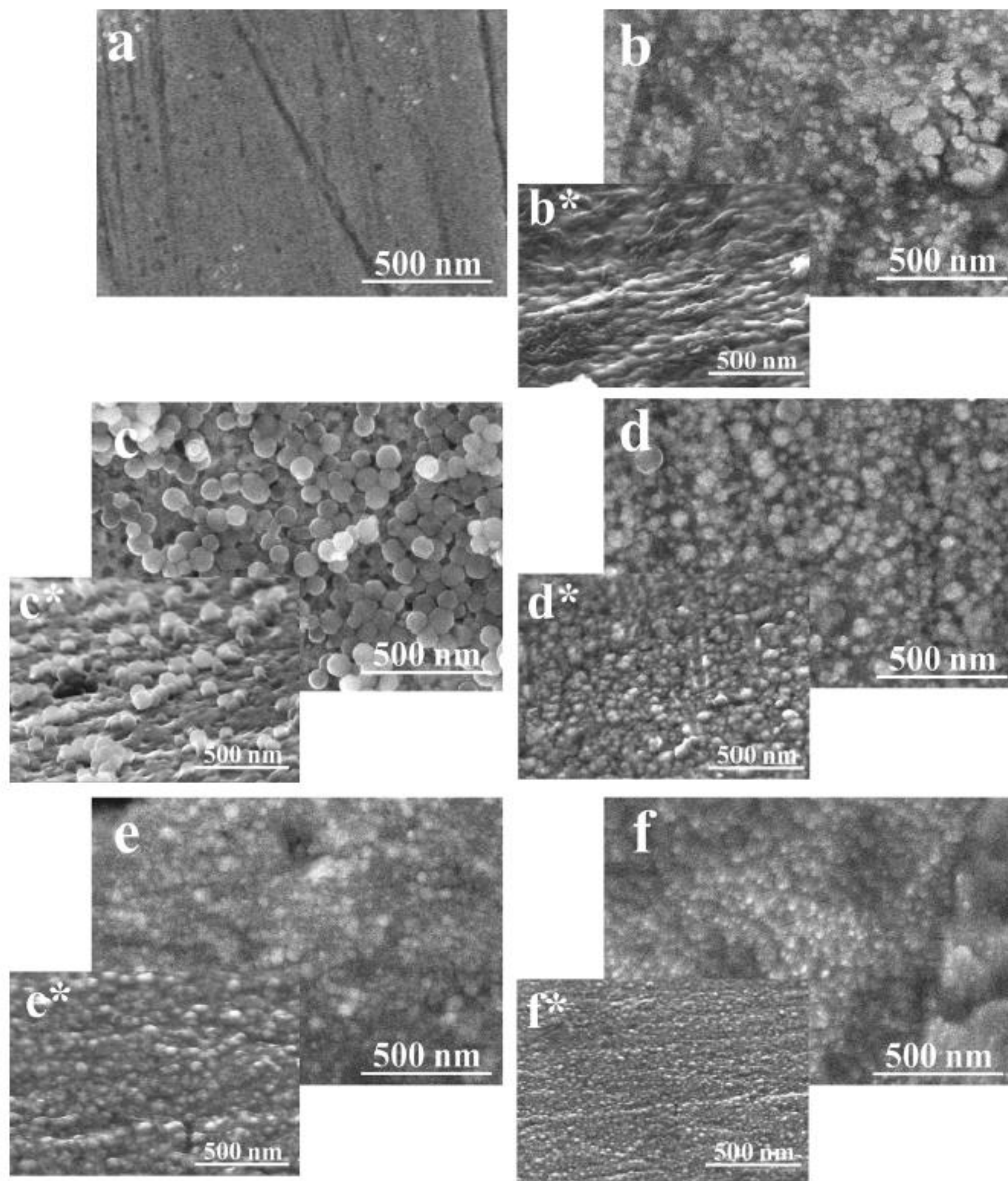

Fig. 5. (a) As-prepared Cu substrate, (b–f) top-view and (b*–f*) side-view SEM images of Cu–Sn coatings deposited at potential of −50 mV for 0.8 s from the sulphate electrolyte containing (b) 0; (c) 0.001; (d) 0.003; (e) 0.005; and (f) 0.010 g/L of TU.

From a practical point of view, galvanostatic deposition is more favorable and common. To further examine the effect of TU on the electrodeposition of Cu–Sn alloy under galvanostatic conditions, chronopotentiometry measurements were performed at the cathodic current density of 0.014 A/cm^2. This current density exceeds the DLC value of the reduction of copper ions estimated from LSV. The results obtained in the electrolyte containing individually Cu^{2+}, as well as both Cu^{2+} and Sn^{2+} ions are summarized in Fig. 6a and Fig. 6b, respectively. In the case of copper electrodeposition (Fig. 6a), a sharp increase in the deposition potential to –480 mV is observed after 30–35 s of electrolysis, which is due to a copper ions depletion in the near electrode area. Further, the cathodic process occurs in the region of hydrogen evolution [33]. In the case of the solution containing both copper and stannous ions (Fig. 6b), a much smaller potential shift was recorded after 25 s of deposition. The electrode potential reaches –40–(–90) mV that corresponds to the range of the UPD of tin. Moreover, potential maxima, observed on *E–t* dependences in the first seconds of electrolysis grow with the increase in TU concentration from 0 to 0.010 g/L. Therefore, these maxima can be assigned to the crystallization overpotential due to the TU adsorption on the electrode surface with the formation of an additional energy barrier.

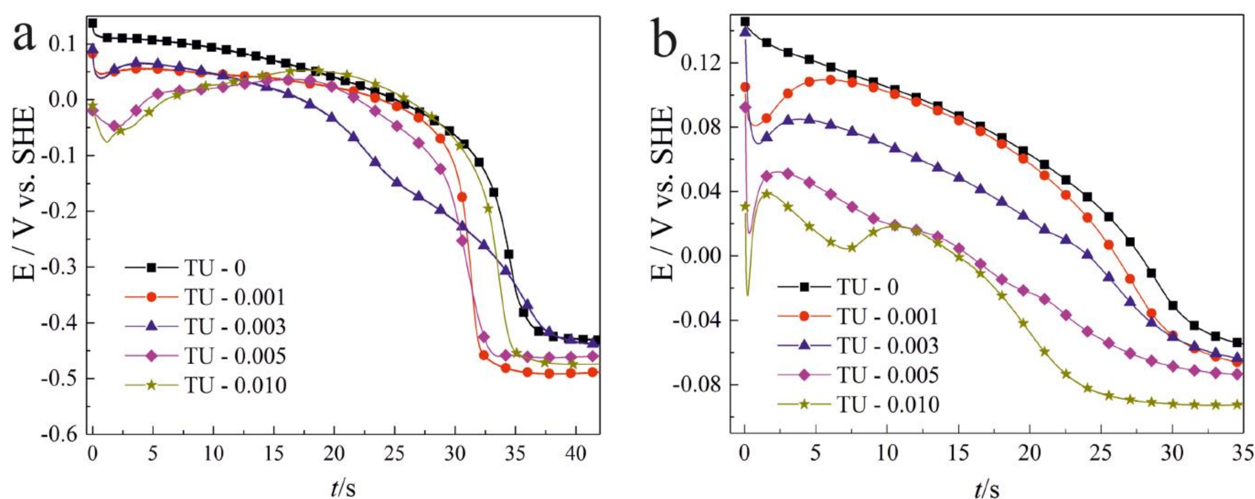

Fig. 6. Chronopotentiograms of copper electrode in sulphate electrolyte containing (a) only Cu^{2+} and (b) simultaneously Cu^{2+} and Sn^{2+} ions with and without TU.

The obtained chronopotentiograms give evidence that only copper is deposited on the cathode's surface in the first seconds of the galvanostatic process. Subsequently, the co-deposition of copper and tin is only possible when the concentration of copper ions at the electrode/electrolyte interface reach diffusion limitations (transition time τ is achieved). To confirm this conclusion, pulse galvanostatic electrolysis at the cathodic current density of 0.014 A/cm^2 was performed from the electrolyte containing both Cu^{2+} and Sn^{2+} ions, as well as 0.001 g/L of TU, following with EDX analysis of formed coatings. Based on the evaluation of the chronopotentiograms, deposition time (pulse duration) was set to 20 and 28 s (Fig. 7a and 7b, respectively), and the pause time was 120 s. To ensure that the thickness of the film is enough for the EDX analysis, 10 pulse-pause deposition cycles were performed. The EDX data revealed that the coating obtained with the pulse duration of 20 s consists only of copper, while that obtained for 28 s is the copper-tin alloy (96.3 wt% Cu–3.7 wt% Sn). Thus, EDX analysis gives evidence of the two-stage process of the Cu–Sn alloy electrodeposition from the sulphate electrolyte at potentials higher than –140 mV.

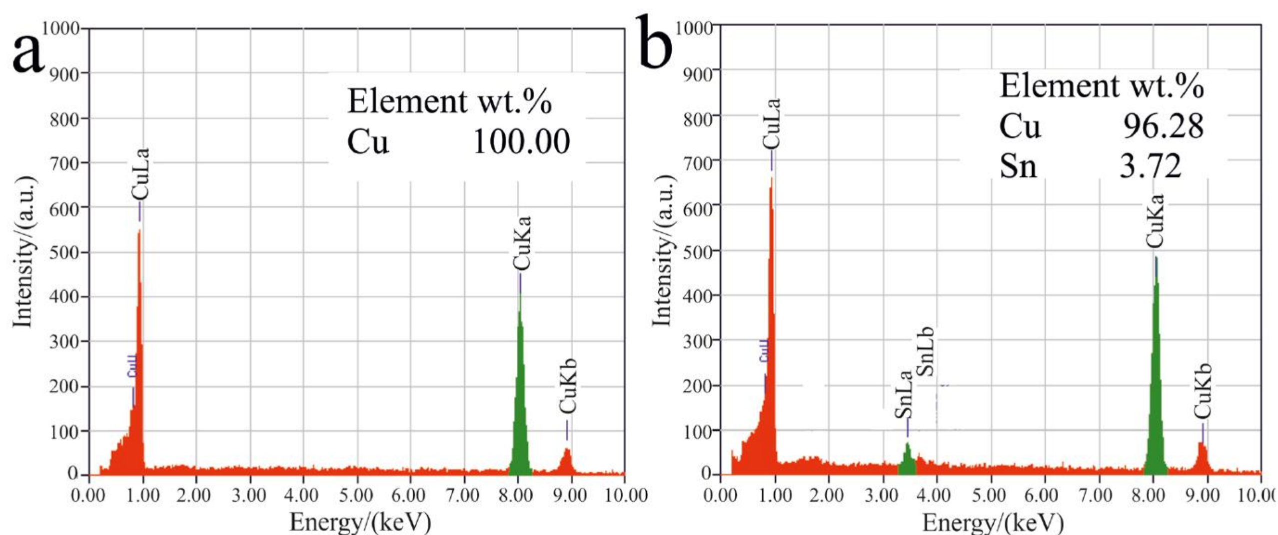

Fig. 7. EDX spectra of coatings deposited from the sulphate electrolyte containing Cu^{2+} and Sn^{2+} ions and 0.010 g/L of TU. Cathodic current density of 0.014 A/cm^2, impulse duration of (a) 20 s and (b) 28 s.

Summarizing the results of potentiostatic and galvanostatic experiments, the following mechanism of the electrochemical deposition of Cu–Sn from the sulphate electrolyte with TU addition at current loads exceeding the limiting diffusion current of copper ions can be proposed (Fig. 8).

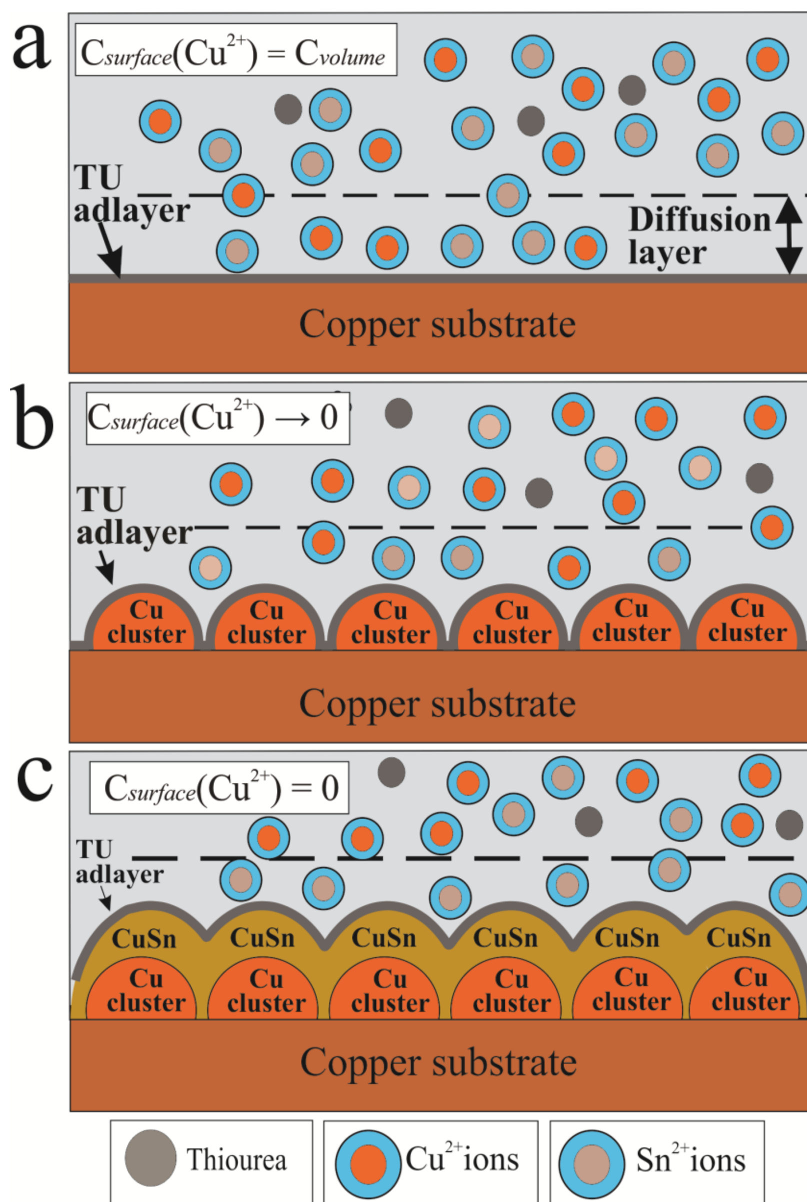

Fig. 8. Schematic illustration of the deposition mechanism of Cu–Sn alloy in the sulphate electrolyte containing TU.

It is known that adsorption of thiourea on copper in acidic media is characterized by negative values of the free Gibbs energy, i.e. is spontaneous [53]. When the cathode is immersed into the deposition bath (no current is passing through the system), a thin adlayer of TU is formed on its surface (Fig. 8a). Considering low TU/(Cu^{2+} + Sn^{2+}) ratios used in this study, metal ions in the bulk solution are presented primarily as aquated cations. Our electrochemical results show that reduction of copper is the initial step of the electrodeposition of Cu–Sn alloy in the region of the UPD of tin. The adsorbed layer of TU or Cu-TU complexes inhibit the reduction process of copper ions. In the first moment of electrolysis, 3D clusters of copper are starting to form on the cathode surface. The following growth of the formed Cu clusters increases the coverage of the electrode surface. Then, the diffusion limitation of copper ions reduction (concentration of copper ions in the near-electrode area strives towards 0, $C_s(Cu^{2+})\rightarrow 0$) is reached (Fig. 8b). At this moment of time $C_s(Cu^{2+}) = 0$, leading to the UPD of tin on the surface of the formed copper clusters (Fig. 8c)."

3.3. Surface morphology of Cu–Sn coatings

Figure 9 shows SEM images of the 13 μm-thick Cu–Sn coatings obtained at the deposition potential of –50 mV from the studied sulphate electrolyte with varying TU content. Rough, large-crystalline coatings were formed from the electrolyte without TU (Fig. 9a). Such morphology can be explained by the continuous growth of the initially formed clusters without the formation of new ones. This results in a nonuniform microstructure of the coating formed. In the case when 0.001 g/L of TU was added to the electrolyte, a decrease in the size of crystallites is clearly visible (Fig. 9b). Only few large crystallites can be seen on SEM image. Moreover, a further increase in the TU concentration up to 0.010

g/L (Fig. 9c–e) promotes the formation of smooth coatings. These observations support the positive effect of TU on the microstructure of the formed alloy.

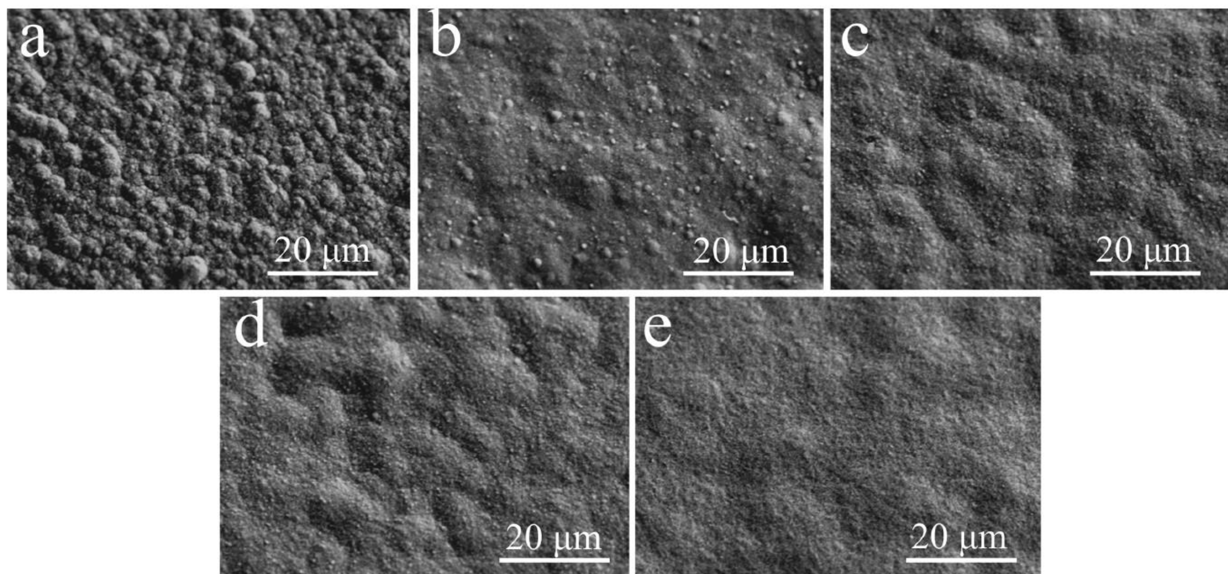

Fig. 9. SEM images of Cu–Sn coatings deposited at −50 mV for 40 min from the sulphate electrolyte containing (a) 0; (b) 0.001; (c) 0.003; (d) 0.005; and (e) 0.010 g/L of TU.

Coatings shown in Fig. 9 were also analyzed using EDX (Table 2). In this case, their thickness (6 µm) was enough to ensure that the measured composition of the coating was not affected by the substrate material. The matte, pink coatings formed from the TU-free electrolyte contain up to 10.14 wt% Sn. The introduction of 0.001 g/L of TU contributes to the increase in the tin content of up to 12.78 wt%. However, a notable gradual decrease in the tin content from 12.78 to 11.68 wt% was observed upon increasing TU concentration up to 0.010 g/L. This changing of the coating composition may have come from the difference in the kinetics of the UPD of Sn, caused by the adsorption of TU on the surface of the electrode. However, it is possible that TU partially decomposes during electrolysis and a very thin

inhomogeneous layer of CuS and SnS sulfides is formed on the alloy surface,[54] which we were not able to detect by either EDX or XPS.

Table 2. EDX analysis of Cu–Sn coatings (thickness of 13 μm) deposited at the potential of −50 mV for 40 min

Thiourea content, g/L	Composition, wt%	
	Cu	Sn
0	89.86 ± 0.24	10.14 ± 0.24
0.001	87.22 ± 0.17	12.78 ± 0.17
0.003	88.01 ± 0.46	11.99 ± 0.46
0.005	88.16 ± 0.31	11.84 ± 0.31
0.010	88.32 ± 0.49	11.68 ± 0.49

In order to quantitatively describe the effect of TU on the roughness of the formed coatings, AFM topography images were obtained (Fig. 10). For the as-prepared Cu substrate calculated R_a was 20 nm (Fig. 10). As expected from SEM observations, Cu–Sn coatings electrodeposited from the electrolyte without TU are characterized by the highest R_a, which was found to be 275 nm. In the case when electrolyte contained TU in the concentration of 0.001, 0.003, 0.005, and 0.010 g/L, the measured R_a was 41, 28, 16, and 9 nm, respectively.

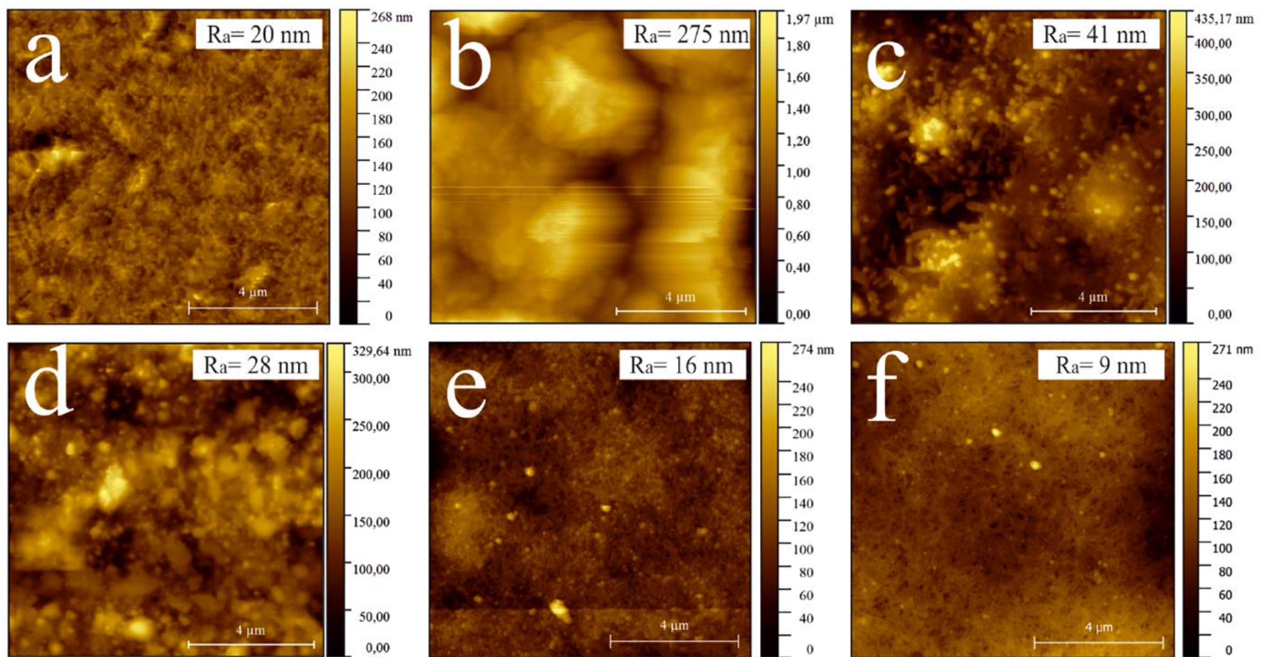

Fig. 10. AFM topography images of (a) Cu substrate and Cu–Sn coatings deposited at −50 mV for 40 min from the sulphate electrolyte containing (b) 0; (c) 0.001; (d) 0.003; (e) 0.005; and (f) 0.010 g/L of TU.

3.4. Phase composition of Cu–Sn coatings

As reported elsewhere [11,13,20], Cu–Sn coatings electrochemically deposited from sulphate electrolytes contain phases that are thermodynamically stable only at high temperatures. X-ray diffraction patterns of Cu–Sn coatings obtained on a polycrystalline copper substrate are presented in Fig. 11. The diffraction peaks of the coatings obtained from solutions containing TU are slightly shifted towards lower 2θ angles as compared to pure Cu (JCPDS 4-368). This shift testifies a slight increase in the interplanar spacing due to the impregnation of tin atoms and the formation of the α-CuSn phase. Average crystallite size ranges from 69 to 83 Å. The sharp peaks confirm the highly crystalline nature of ceria.

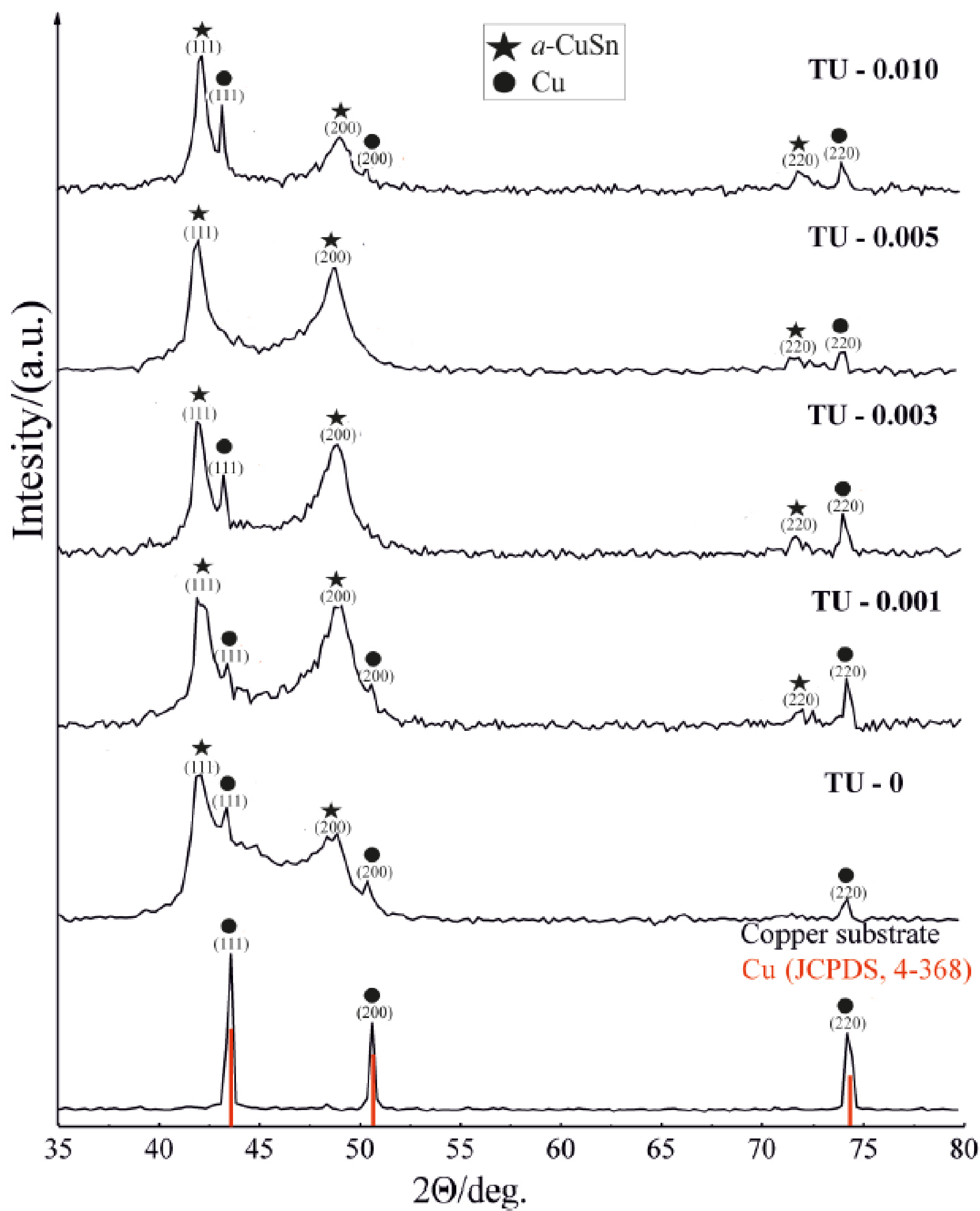

Fig. 11. XRD patterns of copper substrate and Cu–Sn coatings deposited at −50 mV for 40 min from the sulphate electrolyte with and without TU. Spectra are vertically shifter for the ease of comparison

4. Conclusions

Cu–Sn coatings were successfully deposited in either potentiostatic and galvanostatic regimes from sulphate solutions containing TU. The results of linear voltammetry showed that in the concentrations up to 0.010 g/L TU causes pronounced inhibitory effect only on the reduction of copper ions and co-deposition of copper and tin is possible when copper ions are discharged at the limiting diffusion current. The Cu–Sn alloy is deposited at potentials lower than the standard reduction potentials of the $Sn^{2+}|Sn^{0}$ system. Chronoamperometry studies revealed that the potentiostatic electrodeposition of Cu–Sn from TU-containing solutions proceeds through 3D nucleation of copper with diffusion-controlled growth of clusters. When TU was added to the solution in the amount of 0.001–0.005 g/L, copper nucleates according to instantaneous mechanisms, while progressive nucleation governs copper nucleation at the TU concentration of 0.010 g/L. In the galvanostatic experiments, the UPD of tin was observed on the surface of copper clusters when diffusion limitations of the reduction of copper ions were reached. The introduction of TU has a positive effect on the morphology and average surface roughness of Cu–Sn coatings.

Acknowledgments

The study was financially supported by the Ministry of Education of the Republic of Belarus (grant no. 20192233 “Electrochemical composite coatings with photocatalytic properties, based on tin alloys”).

References

[1] S. Jie, M. Ting-yun, Q. Hui-xuan, L. Qi-song, Electrochemical behaviors and electrodeposition of single-phase Cu-Sn alloy coating in [BMIM]Cl, Electrochim. Acta. 297 (2019) 87–93. doi:10.1016/j.electacta.2018.11.189.

[2] A. Afshar, M. Ghorbani, M. Mazaheri, Electrodeposition of graphite-bronze composite coatings and study of electroplating characteristics, Surf. Coatings Technol. 187 (2004) 293–299. doi:10.1016/j.surfcoat.2004.04.096.

[3] C. Meudre, L. Ricq, J.Y. Hihn, V. Moutarlier, A. Monnin, O. Heintz, Adsorption of gelatin during electrodeposition of copper and tin-copper alloys from acid sulfate electrolyte, Surf. Coatings Technol. 252 (2014) 93–101. doi:10.1016/j.surfcoat.2014.04.050.

[4] M. Jung, G. Lee, J. Choi, Electrochemical plating of Cu-Sn alloy in non-cyanide solution to substitute for Ni undercoating layer, Electrochim. Acta. 241 (2017) 229–236. doi:10.1016/j.electacta.2017.04.170.

[5] I. Makarova, I. Dobryden, D. Kharitonov, A. Kasach, J. Ryl, E. Repo, E. Vuorinen, Nickel-nanodiamond coatings electrodeposited from tartrate electrolyte at ambient temperature, Surf. Coatings Technol. 380 (2019) 125063. doi:10.1016/j.surfcoat.2019.125063.

[6] M.J. Cruz, I. V. Makarova, D.S. Kharitonov, I. Dobryden, A.A. Chernik, M. Grageda, S. Ushak, Corrosion properties of nickel coatings obtained from aqueous and nonaqueous electrolytes, Surf. Interface Anal. 51 (2019) 943–953. doi:10.1002/sia.6683.

[7] Y.S. Hedberg, G. Herting, S. Latvala, K. Elihn, H.L. Karlsson, I. Odnevall, Surface passivity largely governs the bioaccessibility of nickel-based powder particles at human exposure conditions,

Regul. Toxicol. Pharmacol. 81 (2016) 162–170. doi:10.1016/j.yrtph.2016.08.013.

[8] X. Wang, G. Herting, Z. Wei, I. Odnevall Wallinder, Y. Hedberg, Bioaccessibility of nickel and cobalt in powders and massive forms of stainless steel, nickel- or cobalt-based alloys, and nickel and cobalt metals in artificial sweat, Regul. Toxicol. Pharmacol. 106 (2019) 15–26. doi:10.1016/j.yrtph.2019.04.017.

[9] N. Pewnim, S. Roy, Electrodeposition of tin-rich Cu-Sn alloys from a methanesulfonic acid electrolyte, Electrochim. Acta. 90 (2013) 498–506. doi:10.1016/j.electacta.2012.12.053.

[10] T. Nickchi, M. Ghorbani, Pulsed electrodeposition and characterization of bronze-graphite composite coatings, Surf. Coatings Technol. 203 (2009) 3037–3043. doi:10.1016/j.surfcoat.2009.03.029.

[11] A. Survila, Z. Mockus, S. Kanapeckaité, V. Jasulaitiené, R. Jušknas, Codeposition of copper and tin from acid sulphate solutions containing gluconic acid, J. Electroanal. Chem. 647 (2010) 123–127. doi:10.1016/j.jelechem.2010.06.015.

[12] A. Survila, Z. Mockus, Surfactant Effects in Cu-Sn Alloy Deposition, J. Electrochem. Soc. 159 (2012) D296–D302. doi:10.1149/2.084205jes.

[13] A. Survila, Z. Mockus, S. Kanapeckaitė, V. Jasulaitienė, R. Juškėnas, Codeposition of copper and tin from acid sulphate solutions containing polyether sintanol DS-10 and benzaldehyde, J. Appl. Electrochem. 39 (2009) 2021–2026. doi:10.1007/s10800-009-9914-2.

[14] L.N. Bengoa, W.R. Tuckart, N. Zabala, G. Prieto, W.A. Egli, Bronze electrodeposition from an acidic non-cyanide high efficiency electrolyte: Tribological behavior, Surf. Coatings Technol. 253 (2014) 241–248. doi:10.1016/j.surfcoat.2014.05.046.

[15] I. Volov, X. Sun, G. Gadikota, P. Shi, A.C. West, Electrodeposition of copper-tin film alloys for interconnect applications, Electrochim. Acta. 89 (2013) 792–797. doi:10.1016/j.electacta.2012.11.102.

[16] M.R. Buchner, F. Kraus, H. Schmidbaur, Pyrophosphate complexation of Tin(II) in aqueous solutions as applied in electrolytes for the deposition of tin and tin alloys such as white bronze, Inorg. Chem. 51 (2012) 8860–8867. doi:10.1021/ic300782q.

[17] A.N. Correia, M.X. Façanha, P. de Lima-Neto, Cu-Sn coatings obtained from pyrophosphate-based electrolytes, Surf. Coatings Technol. 201 (2007) 7216–7221. doi:10.1016/j.surfcoat.2007.01.029.

[18] C. Zanella, S. Xing, F. Deflorian, Effect of electrodeposition parameters on chemical and morphological characteristics of Cu-Sn coatings from a methanesulfonic acid electrolyte, Surf. Coatings Technol. 236 (2013) 394–399. doi:10.1016/j.surfcoat.2013.10.020.

[19] N. Pewnim, S. Roy, Effect of Fluorosurfactant Additive during Cu-Sn Codeposition from Methanesulfonic Acid, J. Electrochem. Soc. . 162 (2015) D360–D364. doi:10.1149/2.0551508jes.

[20] L.N. Bengoa, P. Pary, M.S. Conconi, W.A. Egli, Electrodeposition of Cu-Sn alloys from a methanesulfonic acid electrolyte containing benzyl alcohol, Electrochim. Acta. 256 (2017) 211–219. doi:10.1016/j.electacta.2017.10.027.

[21] C.T.J. Low, F.C. Walsh, Electrodeposition of tin, copper and tin-copper alloys from a methanesulfonic acid electrolyte containing a perfluorinated cationic surfactant, Surf. Coatings Technol. 202 (2008) 1339–1349. doi:10.1016/j.surfcoat.2007.06.032.

[22] A.A. Kasach, D.S. Kharitonov, V.I. Romanovskii, N.M. Kuz’menok, I.M. Zharskii, I.I. Kurilo, Electrodeposition of Cu-Sn Alloy from Oxalic Acid Electrolyte in the Presence of Amine-

containing Surfactants, Russ. J. Appl. Chem. 92 (2019) 835–841. doi:10.1134/S1070427219060144.

[23] A.A. Kasach, I.I. Kurilo, D.S. Kharitonov, S.L. Radchenko, I.M. Zharskii, Effect of Sonochemical Treatment Modes on the Electrodeposition of Cu–Sn Alloy from Oxalic Acid Electrolyte, Russ. J. Appl. Chem. 91 (2018) 591–596. doi:10.1134/S1070427218040092.

[24] S. Jie, M. Ting-yun, Q. Hui-xuan, L. Qi-song, Preparation of black Cu-Sn alloy with single phase composition by electrodeposition method in 1-butyl-3-methylimidazolium chloride ionic liquids, Mater. Chem. Phys. 219 (2018) 421–424. doi:10.1016/j.matchemphys.2018.08.067.

[25] V. Sudha, M. V. Sangaranarayanan, Underpotential deposition of metals: Structural and thermodynamic considerations, J. Phys. Chem. B. 106 (2002) 2699–2707. doi:10.1021/jp013544b.

[26] S. Szabó, Underpotential deposition of metals on foreign metal substrates, Int. Rev. Phys. Chem. 10 (1991) 207–248. doi:10.1080/01442359109353258.

[27] H. Deligianni, I.C.H. Chang, P.C. Andricacos, Alloying of a Less Noble Metal in Electrodeposited Cu Through Underpotential Deposition, J. Electrochem. Soc. 142 (1995) 2244–2249. doi:10.1149/1.2044281.

[28] R. Asseli, M. Benaicha, S. Derbal, M. Allam, O. Dilmi, Electrochemical nucleation and growth of Zn-Ni alloys from chloride citrate-based electrolyte, J. Electroanal. Chem. 847 (2019) 113261. doi:10.1016/j.jelechem.2019.113261.

[29] L. Elias, K.U. Bhat, A.C. Hegde, Development of nanolaminated multilayer Ni-P alloy coatings for better corrosion protection, RSC Adv. 6 (2016) 34005–34013. doi:10.1039/c6ra01547f.

[30] V. Torabinejad, M. Aliofkhazraei, A.S. Rouhaghdam, M.H. Allahyarzadeh, Tribological properties

of Ni-Fe-Co multilayer coatings fabricated by pulse electrodeposition, Tribol. Int. 106 (2017) 34–40. doi:10.1016/j.triboint.2016.10.025.

[31] A.A. Kasach, I.I. Kurilo, D.S. Kharitonov, S.L. Radchenko, I.M. Zharskii, Sonochemical Electrodeposition of Copper Coatings, Russ. J. Appl. Chem. 91 (2018) 207–213. doi:10.1134/S1070427218020064.

[32] C. Oulmas, S. Mameri, D. Boughrara, A. Kadri, J. Delhalle, Z. Mekhalif, B. Benfedda, Comparative study of Cu–Zn coatings electrodeposited from sulphate and chloride baths, Heliyon. 5 (2019) e02058. doi:10.1016/j.heliyon.2019.e02058.

[33] E.E. Farndon, F.C. Walsh, S.A. Campbell, Effect of thiourea, benzotriazole and 4, 5-dithiaoctane-1, 8-disulphonic acid on the kinetics of copper deposition from dilute acid sulphate solutions, J. Appl. Electrochem. 25 (1995) 574–583. doi:10.1007/BF00573215.

[34] A.R. Despić, V.D. Jović, Electrochemical Deposition and Dissolution of Alloys and Metal Composites-Fundamental Aspects, in: R.E. White, J.O. Bockris, B.E. Conway (Eds.), Mod. Asp. Electrochem. Vol. 17, Springer US, Boston, MA, 1995: pp. 143–232. doi:10.1007/978-1-4899-1724-9_2.

[35] I. V. Mironov, L.D. Tsvelodub, Complexation of copper(I) by thiourea in acidic aqueous solution, J. Solution Chem. 25 (1996) 315–325. doi:10.1007/BF00972529.

[36] N. Tantavichet, M.D. Pritzker, Aspects of copper electrodeposition from acidic sulphate solutions in presence of thiourea, Trans. IMF. 84 (2006) 36–46. doi:10.1179/174591906X10529.

[37] F. Kesri, A.M. Affoune, I. Djaghout, Effects of thiourea on the kinetics and electrochemical nucleation of tin electrodeposition from stannous chloride bath in acidic medium, J. Serbian Chem.

Soc. 84 (2019) 41–53. doi:10.2298/JSC180325107K.

[38] L.A. Azpeitia, C.A. Gervasi, A.E. Bolzán, Effects of Temperature and Thiourea Addition on the Electrodeposition of Tin on Glassy Carbon Electrodes in Acid Solutions, Electrochim. Acta. 257 (2017) 388–402. doi:https://doi.org/10.1016/j.electacta.2017.10.064.

[39] J. Ustarroz, J.A. Hammons, T. Altantzis, A. Hubin, S. Bals, H. Terryn, A generalized electrochemical aggregative growth mechanism, J. Am. Chem. Soc. 135 (2013) 11550–11561. doi:10.1021/ja402598k.

[40] M.H. Mamme, C. Köhn, J. Deconinck, J. Ustarroz, Numerical insights into the early stages of nanoscale electrodeposition: Nanocluster surface diffusion and aggregative growth, Nanoscale. 10 (2018) 7194–7209. doi:10.1039/c7nr08529j.

[41] D. Grujicic, B. Pesic, Reaction and nucleation mechanisms of copper electrodeposition from ammoniacal solutions on vitreous carbon, Electrochim. Acta. 50 (2005) 4426–4443. doi:https://doi.org/10.1016/j.electacta.2005.02.012.

[42] M.H. Hoizle, C.W. Apsel, T. Will, D.M. Kolb, Copper Deposition onto Au(111) in the Presence of Thiourea, J. Electrochem. Soc. 142 (1995) 3741–3749. doi:10.1149/1.2048407.

[43] M.B. Quiroga Argañaraz, C.I. Vázquez, G.I. Lacconi, Copper electrodeposition onto hydrogenated Si(1 1 1) surfaces: Influence of thiourea, J. Electroanal. Chem. 639 (2010) 95–101. doi:10.1016/j.jelechem.2009.11.028.

[44] V.A. Isaev, Y.P. Zaykov, O. V Grishenkova, A. V Kosov, O.L. Semerikova, Analysis of Potentiostatic Current Transients for Multiple Nucleation with Diffusion and Kinetic Controlled Growth, J. Electrochem. Soc. 166 (2019) D851–D856. doi:10.1149/2.1061915jes.

[45] V.A. Isaev, O. V. Grishenkova, Y.P. Zaykov, On the theory of 3D multiple nucleation with kinetic controlled growth, J. Electroanal. Chem. 818 (2018) 265–269. doi:10.1016/j.jelechem.2018.04.051.

[46] L. Guo, G. Oskam, A. Radisic, P.M. Hoffmann, P.C. Searson, Island growth in electrodeposition, J. Phys. D. Appl. Phys. 44 (2011). doi:10.1088/0022-3727/44/44/443001.

[47] A. Milchev, Electrocrystallization: Nucleation and growth of nano-clusters on solid surfaces, Russ. J. Electrochem. 44 (2008) 619–645. doi:10.1134/S1023193508060025.

[48] B. Scharifker, G. Hills, Theoretical and experimental studies of multiple nucleation, Electrochim. Acta. 28 (1983) 879–889.

[49] M.E. Hyde, R.G. Compton, A review of the analysis of multiple nucleation with diffusion controlled growth, J. Electroanal. Chem. 549 (2003) 1–12. doi:10.1016/S0022-0728(03)00250-X.

[50] Y. Liu, L. Wang, K. Jiang, S. Yang, Electro-deposition preparation of self-standing Cu-Sn alloy anode electrode for lithium ion battery, J. Alloys Compd. 775 (2019) 818–825. doi:10.1016/j.jallcom.2018.10.207.

[51] K.S. Kumar, K. Biswas, Effect of thiourea on grain refinement and defect structure of the pulsed electrodeposited nanocrystalline copper, Surf. Coatings Technol. 214 (2013) 8–18. doi:https://doi.org/10.1016/j.surfcoat.2012.10.018.

[52] A. Radisic, P.M. Vereecken, J.B. Hannon, P.C. Searson, F.M. Ross, Quantifying Electrochemical Nucleation and Growth of Nanoscale Clusters Using Real-Time Kinetic Data, Nano Lett. 6 (2006) 238–242. doi:10.1021/nl052175i.

[53] A. Łukomska, S. Smoliński, J. Sobkowski, Adsorption of thiourea on monocrystalline copper electrodes, Electrochim. Acta. 46 (2001) 3111–3117. doi:https://doi.org/10.1016/S0013-

4686(01)00602-8.

[54] M.S. Kang, S.K. Kim, K. Kim, J.J. Kim, The influence of thiourea on copper electrodeposition: Adsorbate identification and effect on electrochemical nucleation, Thin Solid Films. 516 (2008) 3761–3766. doi:10.1016/j.tsf.2007.06.069.